Quantum dots-templated growth of strain-relaxed GaN on a *c*-plane sapphire by radio-frequency molecular beam epitaxy*

Guo Hao-Min(郭浩民), Wen Long(文 龙), Zhao Zhi-Fei(赵志飞), Bu Shao-Jiang(步绍姜), Li Xin-Hua(李新化)†, and Wang Yu-Qi(王玉琦)

Key Laboratory of Materials Physics, Institute of Solid State Physics, Chinese Academy of Sciences, Hefei 230031, *China*

(Received 30 March 2012; revised manuscript received 18 April 2012)

We investigated the quantum dots-templated growth of a (0001) GaN film on a *c*-plane sapphire substrate. The growth was carried out in a radio-frequency molecular beam epitaxy system. The enlargement and coalescence of grains on the GaN quantum dots template was observed in the atom force microscopy images, as well as the more ideal surface morphology of the GaN epitaxial film on the quantum dots template compared with the one on the AlN buffer. The Ga polarity was confirmed by the reflected high energy electron diffraction patterns and the Raman spectra. The significant strain relaxation in the quantum dots-templated GaN film was calculated based on the Raman spectra and the X-ray rocking curves. Meanwhile, the threading dislocation density in the quantum dots-templated film was estimated to be 7.1×10^7 cm^{-2}, which was significantly suppressed compared with that of the AlN-buffered GaN film. The room-temperature Hall measurement showed an electron mobility of up to 1860 cm^2/V$\cdot$s in the two-dimensional electron gas at the interface of the $Al_{0.25}Ga_{0.75}N$/GaN heterojunction.

Keywords: III–V semiconductor, radio-frequency molecular beam epitaxy, dislocation

PACS: 81.05.Ea, 81.15.Hi, 61.72.Hh **DOI:** 10.1088/1674-1056/21/10/108101

1. Introduction

The GaN material has potential applications in optical devices as well as high-power and high-frequency electronic devices due to its wide bandgap, high thermal conductivity, and the high saturation velocity of electrons,[1−3] which has attracted great interest in the past two decades. While great progress has been made in the growth of high quality materials, further developments in this area are necessary in order to provide wafers that have Ga polarity, smooth surfaces, and low density threading dislocations (TDs).[4,5]

Due to the lack of suitable substrates, nitride epitaxial layers are generally grown on SiC or sapphire wafers. Many researchers have demonstrated that GaN films grown on *c*-plane sapphire substrates show Ga polarity with the employing of high-temperature AlN buffer layers.[6−8] However, due to the significant biaxial strain caused by the substantial mismatch in the lattice constant and thermal conductivity between the substrate and the epitaxial layer, lattice defects such as TDs will be incorporated. These lattice defects have been reported to be electrically active and can therefore contribute to trapping and recombination within the device structure, leading to the degradation in the output characteristics of the device.[9,10]

To reduce the biaxial strain and eliminate the lattice defects of GaN films, many practical methods have been applied. For example, the methods based on the epitaxial lateral overgrowth (ELO) have been commonly used to obtain high quality GaN films.[11−13] However, the ELO fabrication is complicated in the photolithography step. Moreover, unintentionally incorporated carbon impurities will result in the decline of the crystal quality. Recently, the nanoscale epitaxial lateral overgrowth (NELO) of GaN films on nanoscale arrays has shown its superiority in suppressing the TD density, since the nanoscale arrays act as a strain-relaxed buffer for the lateral overgrowth of low-TD-density GaN epitaxial layers without any interruption during the growth.[14−16] Never-

*Project supported by the National Natural Science Foundation of China (Grant No. 1179042).

†Corresponding author. E-mail: xinhuali@issp.ac.cn

© 2012 Chinese Physical Society and IOP Publishing Ltd

theless, the nanoscale arrays in most reports were prepared by using the metal-catalyzed vapor–liquid–solid mode. The metal catalyst droplets were deposited on the substrates prior to the growth, and they were likely to be buried in the GaN films during the lateral overgrowth, which might affect the device properties.[15] In order to resolve this problem, it is necessary to develop an *in-situ* growth method without any pre-treatments and growth interruptions.

Quantum dots (QDs) may be a suitable candidate. On the one hand, defect-free QDs can be easily fabricated by using the self-assembled method, and no metal catalyst is needed; on the other hand, the formation of QDs will lead to strain relaxation.[17−19] That is to say, the epitaxial growth on QDs will benefit from the strain relaxation and not suffer from any growth interruption. In this study, we report on the growth of GaN epitaxial layers on a self-assembled GaN QDs template by radio-frequency molecular beam epitaxy (RF-MBE). The influences of the GaN QDs template on the surface morphologies, biaxial strains, TD densities, and electrical properties of the GaN epitaxial layers are studied.

2. Experimental details

GaN layers were grown on 2-inch (0001) sapphire substrates by RF-MBE in a modified Varian GEN-II system. The Ga and Al fluxes were supplied by standard effusion cells. Electrically neutral nitrogen atoms were obtained from an SVTA radio-frequency plasma-assisted source (Model 4.35) with a 700-V voltage used to deflect the active nitrogen ions. The intensity of the nitrogen atom beam was evaluated based on the plasma photocurrent measured by a detector. Following the degasification at 900 °C, the substrate was nitridated at 200 °C for 1 h, and the nitrogen plasma source power and photocurrent were fixed at 300 W and 16 μA, respectively. A 100-nm thick AlN buffer layer was then deposited at 850 °C with the growth interruption modulation of the Al cell under a fixed nitrogen plasma source power and photocurrent of 180 W and 8 μA, respectively. The Al flux was kept at 2.6×10^{-7} Torr (1 Torr = 1.33322×10^2 Pa) with the computer-controlled shutter open and closed periodically. The growth time was 30 s and the annealing time was 10 s in one period. Then the substrate temperature was lowered to 780 °C, and GaN QDs were grown through the modified S–K mode. In this mode, 5-monolayers (MLs) GaN was first deposited under Ga-rich conditions. At this step, the Ga flux was fixed at 4×10^{-7} Torr; and the nitrogen plasma source power and photocurrent were increased to 300 W and 16 μA, respectively. Afterwards, a growth interruption was carried out for the evaporation of excess Ga and the subsequent rearrangement of the two-dimensional (2D) layer into three-dimensional (3D) dots. Finally, under constant nitrogen flux and temperature, the Ga flux was increased to 8×10^{-7} Torr for the growth of GaN films.

In order to study the effect of the growth duration on the surface morphology, a series of samples with different growth times were synthesized. Meanwhile, another sample of the same thickness was directly deposited on the AlN buffer for comparison with the QDs-templated samples. Additionally, $Al_{0.25}Ga_{0.75}N$/GaN heterojunctions were prepared with a 30-nm-thick $Al_{0.25}Ga_{0.75}N$ barrier layer each deposited on the QDs-templated and the AlN-buffered GaN films.

The surface morphology was characterized by a Veeco AutoProbe CP using atom force microscopy (AFM). X-ray rocking curves (XRCs) were measured using a Philips X'pert diffractormeter (X'pert-pro MPD) with Cu K_α radiation. Raman analysis was carried out in back scattering geometry at room temperature (RT) using the polarized 514.5-nm line of an argon-ion laser in an LABRAM-HR system.

3. Results and discussion

The reflection high-energy electron diffraction (RHEED) patterns observed during the growth are shown in Fig. 1. As shown in Fig. 1(a), the streaky 1×1 RHEED pattern (top) of the as-grown AlN buffer layer is dim for the thin Al adlayer and Al droplets on the surface. The RHEED pattern (bottom) becomes brighter when annealing in the N plasma, which is attributed to the sufficient diffusion of Al atoms and the reaction between Al and N atoms on the surface. In this case, the surface of the AlN buffer layer is smooth, and no Al droplets are found. Additionally, the RHEED pattern maintains streaks 1×1 when the Al flux is closed, revealing the Al polarity of the AlN buffer layer, which ensures the Ga polarity of the following GaN film. Figure 1(b) shows a streaky 1×1 RHEED pattern (top), which indicates the two-dimensional (2D) growth mode of the 5-ML

GaN layer. The pattern transforms to a spotty one (bottom) during the growth interruption, indicating the transition to three-dimensional (3D) growth mode of GaN QDs.[17,18] The RHEED pattern of the QDs-templated GaN layer is shown in Fig. 1(c). A brighter streaky 2×2 pattern with dim 1/2-order streaks is observed once the sample temperature drops to about 400 °C. The 2 × 2 reconstruction keeps visible with the further decrease of temperature to RT, revealing the Ga polarity of the GaN film.

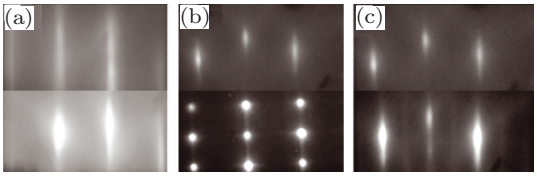


Fig. 1. RHEED patterns of the AlN buffer layer, GaN QDs template, and GaN film: (a) the as-grown AlN buffer layer (top) and the buffer layer *in-situ* annealing (bottom); (b) a 5-ML-thick GaN layer (top) and GaN QDs (bottom); (c) the as-grown QDs-templated GaN film (top) and the GaN film *in-situ* annealing at 400 °C (bottom).

Surface morphologies obtained by AFM are shown in Figs. 2(a)–2(d). Figure 2(a) displays a 1 μm × 1 μm image of the GaN QDs template (sample A). High density GaN QDs are observed with average diameter and height estimated to be 16 nm and 4 nm, respectively. For the initial 10-min growth (sample B), near hexagon shaped grains are observed, as shown in Fig. 2(b), indicating the lateral growth on QDs. The average diameter and height of the grains are estimated to be 78 nm and 17 nm, respectively, thus the horizontal and the vertical growth rates are approximately 3 nm and 1.3 nm per minute, respectively. The dominant lateral growth is attributed to the higher growth rate on the QD facets of high index planes compared to the *c*-plane.[17] It is noteworthy that only part of the QDs display lateral growth, which may be attributed to the different deposition modes of the QDs. Most GaN QDs are likely to be preferentially located at TDs originated from the AlN buffer due to their low energies as nucleation sites, while a minority may also nucleate in areas that are free of TDs.[19] The QDs at TDs tend to grow faster than the TD-free ones due to the lower energy cost associated with the addition of atoms to a strain-relaxed lattice. When the growth time is extended to 30 min, as shown in Fig. 2(c), the QDs located at TDs grow into higher and larger grains, and the grains coalesce and cover the TD-free QDs. The average diameter of the larger grains is about 1.5 μm, while the thickness is about 300 nm. Nevertheless, a considerable number of pits are still observed. The 5 μm × 5 μm AFM image of a 800-nm-thick GaN film grown for 60 min (sample D) is shown in Fig. 3(d), showing a smooth (RMS roughness = 0.6 nm) and nearly pit-free surface. In contrast, the pitted surface (RMS roughness = 1.4 nm) of the directly grown GaN layer (sample E) on the AlN buffer layer is observed in Fig. 2(e).

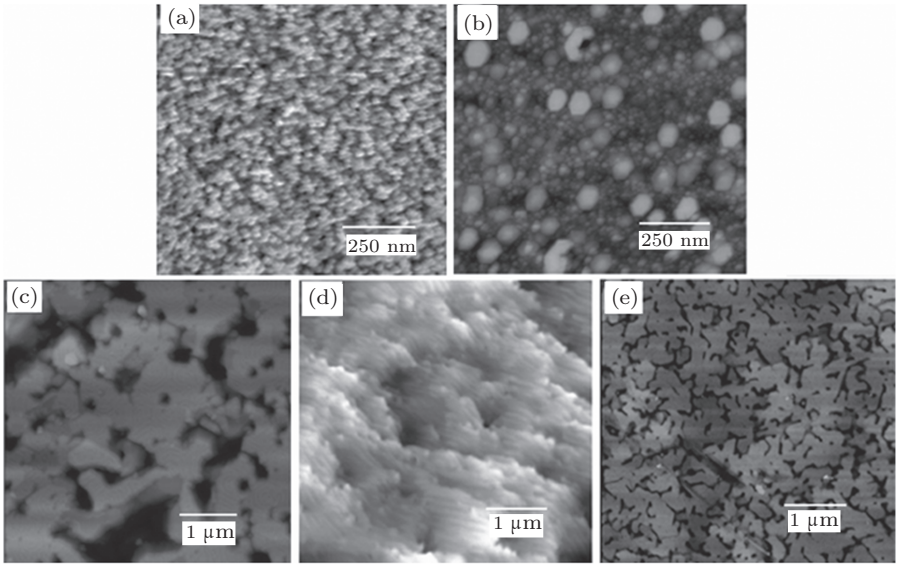


Fig. 2. AFM images of (a) sample A: the GaN QDs template (1 μm × 1 μm), (b) sample B: grown for 10 min (1 μm × 1 μm), (c) sample C: a 300-nm-thick GaN layer grown for 30 min (5 μm × 5 μm), (d) sample D: an 800-nm-thick GaN layer grown for 60 min (5 μm × 5 μm), and (e) sample E: an 800-nm-thick GaN layer directly grown on AlN buffer (5 μm × 5 μm).

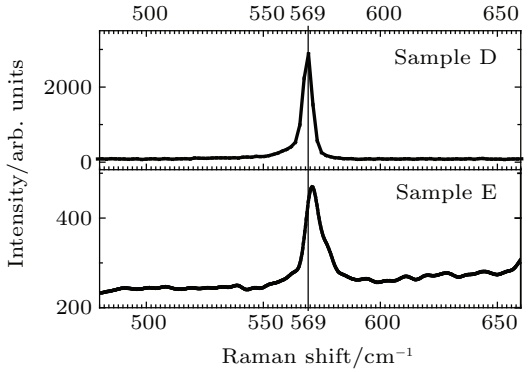


Fig. 3. The E_2 (high) modes observed in the RT Raman analysis for samples (a) D and (b) E.

The Raman analysis is carried out at RT in a backscattering geometry with the incident light along the c axis, which is a $-z(y, xy)z$ geometry. As shown in Fig. 3 the E_2 (high) modes of samples D and E are observed at 569.308 cm^{-1} and 570.760 cm^{-1}, respectively, while the standard strain-free value is 569 cm^{-1} as reported in Ref. [20]. As Peng *et al.* presented, the E_2 (high) mode can be shifted only by the compressive stress; meanwhile, the Ga-polar GaN specimens show compressive stresses, while the tensile stresses exist in N-polar ones.[21] Accordingly the frequency shifts in our samples indicate their compressive stresses and Ga polarity. Goni *et al.* have reported that the Raman frequency shift $\Delta\omega$ obeys the equation

$$\sigma = \Delta\omega/4.24 \text{ (GPa)}, \quad (1)$$

where σ is the biaxial strain.[22] Based on Eq. (1), the in-plane compressive stresses in samples D and E are estimated at 0.073 GPa and 0.415 GPa, respectively. From the results, we can see that the in-plane compressive stress is efficiently relaxed in the QDs-templated growth for sample D.

The XRCs of (0002) symmetry planes and (10-12) asymmetry planes of samples D and E are shown in Figs. 4(a) and 4(b), respectively. The peak positions of the curves are given in the figures as well. The lattice constants are evaluated by Bragg's law to be $a = 0.31885$ nm, $c = 0.51854$ nm for sample D and $a = 0.31863$ nm, $c = 0.51872$ nm for sample E. The lattice constants of sample D are very close to those of the strain-free film ($a_0 = 0.3189$ nm, $c_0 = 0.5185$ nm reported by Ref. [23]), while larger deviations are discovered for sample E. The in-plane biaxial compressive stress σ_a in the GaN sample satisfies the relationship

$$\sigma_a = M\varepsilon_a, \quad (2)$$

where M is the biaxial elastic modulus, and ε_a is the in-plane deformation. The in-plane biaxial compressive stress can be calculated by using $M = 449$ GPa and $\varepsilon_a = (a - a_0)/a_0$.[24] Therefore, the in-plane biaxial compressive stress in samples D and E can be calculated to be 0.070 GPa and 0.380 GPa, respectively, which are quite consistent with the results obtained from Raman spectra.

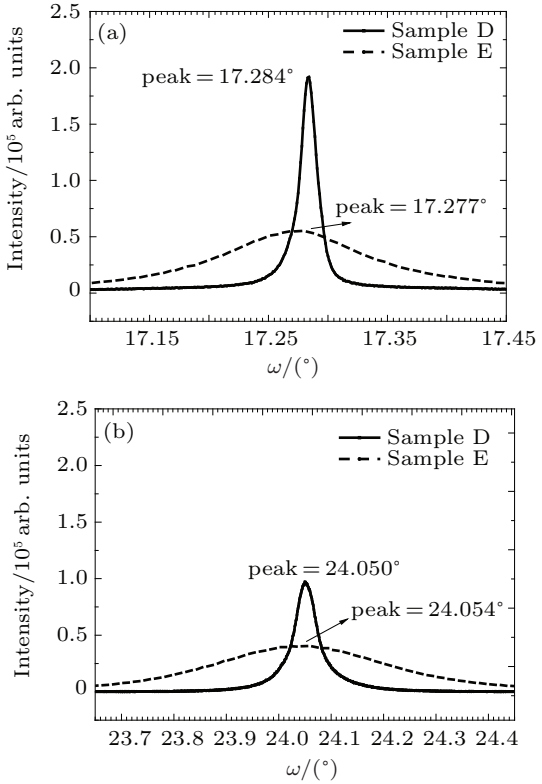


Fig. 4. XRCs of samples D and E for (a) (0002) symmetry plane and (b) (10-12) asymmetry planes.

The TD densities in the GaN films are estimated by the following equations

$$D_{\text{screw}} = \beta^2_{(0002)}/(9b^2_{\text{screw}})_{\text{edge}} = \beta^2_{(10-12)}/(9b^2_{\text{edge}}), \quad (3)$$

where D_{screw} and D_{edge} are the densities of the screw and the edge dislocations, respectively, b is the Burgers vector length ($b_{\text{screw}} = 0.5185$ nm and $b_{\text{edge}} =$ 03189 nm),[25] $\beta_{(0002)}$ and $\beta_{(10-12)}$ are the values of the full width at half maximum (FWHM) of the (0002) and (10-12) planes, which reflect the screw and edge dislocation densities, respectively.[26–28] The calculated FWHMs for the (0002) and (10-12) planes of sample D are 61.2 arcsec and 180 arcsec, respectively, while they are 558 arcsec and 1404 arcsec for sample E, respectively. According to Eq. (3), the TD densities are evaluated to be

Sample D: $D_{\text{screw}} \approx 4.6 \times 10^6$ cm^{-2}, $D_{\text{edge}} \approx 6.6 \times 10^7$ cm^{-2}, $D_{\text{TDs}} \approx 7.1 \times 10^7$ cm^{-2};

Sample E: $D_{\text{screw}} \approx 1.0 \times 10^8$ cm^{-2}, $D_{\text{edge}} \approx 5.1 \times 10^9$ cm^{-2}, $D_{\text{TDs}} \approx 5.2 \times 10^9$ cm^{-2}.

The results show that the edge dislocations are the major TDs in both samples. The TD density in the QDs-templated GaN film is significantly reduced compared with that in the AlN-buffered GaN film.

The decrease of TD density is mainly attributed to the growth process greatly influenced by the TDs. The TDs in the GaN epitaxial layer can be classed into two types, the TDs spreading into the GaN film from the AlN buffer (type I) and the TDs existing at the grain boundaries (Type II).[19,29] Type I TDs will be beside QDs but will never propagate through them,[19] therefore most TDs of Type I cannot reach the sample surface during the epitaxial process. The QDs beside the Type I TDs grow into higher and larger grains. Due to the coalescence of the grains, the boundaries are significantly reduced, and the density of Type II TDs decreases.[29] Thus, the TD density in the QDs-templated GaN film is correspondingly decreased.

Based on the QDs-templated GaN sample and the directly grown GaN sample on the AlN buffer, the $Al_{0.25}Ga_{0.75}N$/GaN heterojunctions are also prepared. The measured RT Hall mobility and the 2D electron gas (2DEG) sheet density are listed in Table 1. The carrier mobility increases by about 3 times for the QDs-templated sample compared to that of the AlN-buffered sample. The increase in carrier density is also observed. The mobility up to 1860 $cm^2/V \cdot s$ is attributed to the combined effects of the smooth interface and the decrease of TD related electron traps and scattering centers.[30]

Table 1. The RT carrier mobility and density of the two-dimensional electron gas (2DEG).

$Al_{0.25}Ga_{0.75}N$/GaN heterojunction	Carrier density $/10^{13}$ cm^{-2}	Mobility $/(cm^2/V \cdot s)$
Sample D+$Al_{0.25}Ga_{0.75}N$	1.3	1860
Sample E+$Al_{0.25}Ga_{0.75}N$	1.0	594

4. Conclusion

The GaN QDs template is employed as a strain relaxed buffer, on which the high quality Ga-polarity GaN film has been fabricated by RF-MBE. The Ga polarity of all GaN epitaxial films is confirmed by RHEED and Raman analysis. The smooth and pit-free surface of the QDs-templated GaN film is observed by AFM. According to the Raman spectra, the biaxial compressive stress in the QDs-templated film is estimated to be 0.071 GPa, which is only about 19% of the value of the AlN-buffered GaN. Similar values are also given by XRCs. Compared to the sample directly deposited on the AlN buffer, the significantly decreased TD density in the QDs-templated GaN film is estimated to be $D \approx 7.1 \times 10^7$ cm^{-2}. The RT Hall measurement of the $Al_{0.25}Ga_{0.75}N$/GaN heterojunction based on the QDs-templated GaN film displays the electron mobility up to 1860 $cm^2/V \cdot s$ of the 2DEG at the interface, which indicates the QDs-templated growth has a significant improvement on the GaN film quality.

References

[1] Pearton S J, Zolper J C and Shul R J 1999 *J. Appl. Phys.* **86** 1

[2] Mishra U K, Parikh P and Wu Y F 2002 *Proc. IEEE* **90** 1022

[3] Lim Wantae, Jeong Jae-Hyun, Lee Jae-Hoon, Hur Seung-Bae, Ryu Jong-Kyu, Kim Ki-Se, Kim Tae-Hyung, Song Sang Yeob, Yang Jong-In and Pearton S J 2011 *Appl. Phys. Lett.* **97** 242103

[4] Speck J S and Rosner S J 1999 *Physica* B **274** 24

[5] Qiu K, Zhong F, Li X H, Yin Z J, Ji C J, Han Q F, Chen J R, Cao X C and Wang Y Q 2007 *Chin. Phys.* **16** 282

[6] Shen X Q, Ide T, Cho S H, Shimizu M, Hara S, Okumura H, Sonoda S and Shimizu S 2000 *J Cryst. Growth* **218** 155

[7] Smith A R, Feenstra R M, Greve D W, Negebauer J and Northrup J E 1997 *Phys. Rev. Lett.* **79** 3934

[8] Zhong F, Qiu K, Li X H, Yin Z J, Xie X J, Wang Y, Ji C J, Cao X C, Han Q F, Chen J R and Wang Y Q 2007 *Chin. Phys. Lett.* **24** 240

[9] Craven M D, Lim S H, Wu F, Speck J S and DenBaars S P 2002 *Appl. Phys. Lett.* **81** 469

[10] Chakraborty A, Kim K C, Wu F, Speck J S, DenBaars S P and Mishra U K 2006 *Appl. Phys. Lett.* **89** 41903

[11] Seon M, Prokofyeva T and Holtz M 2000 *Appl. Phys. Lett.* **76** 14

[12] Gibart P 2004 *Rep. Prog. Phys.* **67** 667

[13] Okada N, Kawashima Y and Tadatomo K 2008 *Appl. Phys. Express* **1** 111101

[14] Chiu C H, Yen H H, Chao C L, Li Z Y, Yu P C, Kuo H C, Lu T C, Wang C C, Lau K M and Cheng S J 2008 *Appl. Phys. Lett.* **93** 081108

[15] Li Q M, Lin Y, Creighton J R, Figiel J J and Wang G T 2009 *Adv. Mater.* **21** 2416

[16] Ku J T, Yang T H, Chang J R, Wong Y Y, Chou W C, Chang C Y and Chen C Y 2010 *Jpn. J. Appl. Phys.* **49** 04DH06

[17] Gogneau N, Jalabert D and Monroy E 2003 *J. Appl. Phys.* **94** 4

[18] Xu T, Zhou L, Wang Y Y, Özcan A S, Ludwig K F, Smith D J and Moustakas T D 2007 *J. Appl. Phys.* **102** 073517

[19] Simon R J, Pelekanos N, Daudin B and Feuillet G 1999 *Appl. Phys. Lett.* **75** 2639

[20] Zhong F, Li X H, Qiu K, Yin Z J, Ji C J, Cao X C, Han Q F, Chen J R and Wang Y Q 2007 *Chin. Phys.* **16** 2786

[21] Peng C X, Weng H M, Zhu C F, Ye B J, Zhou X Y, Han R D, Fong W K and Surya C 2007 *Physica* B **391** 6

[22] Goni A R, Siegle H, Syassen K, Thomsen C and Wagner J M 2001 *Phys. Rev.* B **64** 035205

[23] Vispute R D and Talyansky V 1997 *Appl. Phys. Lett.* **70** 2735

[24] Wright A F 1997 *J. Appl. Phys.* **82** 2833

[25] Ide T, Shimizu M, Shen X Q, Jeganathan K, Okumura H and Nemoto T 2002 *J. Cryst. Growth* **245** 15

[26] Zheng X H, Chen H, Yan Z B, Han Y J, Yu H B, Li D S, Huang Q and Zhou J M 2003 *J. Cryst. Growth* **255** 63

[27] Perlin P, Jauberthie-Carillon C, Itie J P, Miguel A S, Grzegroy I and Polian A 1992 *Phys. Rev.* B **45** 83

[28] Liu Z Y, Zhang J C, Duan H T, Xue J S, Lin Z Y, Ma J C, Xue X Y and Hao Y 2011 *Chin. Phys.* B **20** 097701

[29] Shimizu M, Chonan H, Piao G X, Okumura H and Nakanishi H 2006 *Mater. Sci. Forum.* **527–529** 1493

[30] Lu L W, Fong W K, Zhu C F, Leung B H, Surya C, Wang J and Ge W 2002 *J. Cryst. Growth* **234** 99